Electronic Supplementary Information (ESI)

Atomic-scale selectivity of hydrogen for storage sites in Pd nanoparticles at atmospheric pressure

Wenjuan Yuan[‡], Mengke Ge[‡],Kai Wang, Xingang Hou, Ning Liu, Ziliang Deng, Ruijie Guo, Siyu Liu, Yunfeng Zhao, Jia He*, Wei Xi*, Jun Luo and Yi Ding

Center for Electron Microscopy and Tianjin Key Laboratory of Advanced Functional Porous Materials, Institute for New Energy Materials & Low-Carbon Technologies, School of Materials Science and Engineering, Tianjin University of Technology,

Tianjin 300384, China

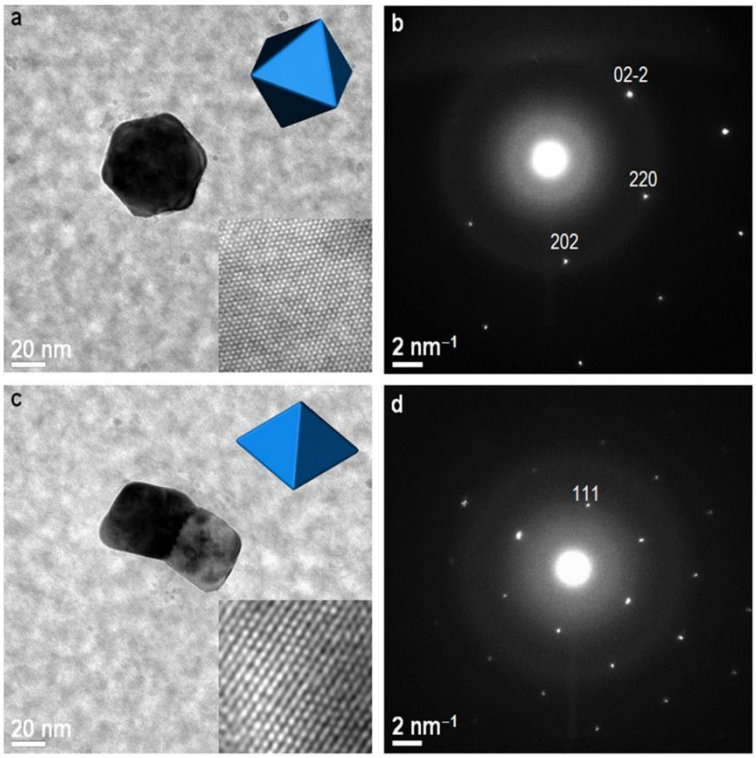

Fig. S1 TEM characterization of Pd octahedral nanoparticles with different orientations. (a) Low-magnification TEM image of a Pd octahedral nanoparticle when its <111> crystal orientation was nearly parallel to the electron beam; the two insets are the 3D schematic and HRTEM images of the nanoparticle. (b) SAED pattern of the nanoparticle in (a). (c) and (d) provide similar information for another nanoparticle when its <110> crystal orientation was nearly parallel to the electron beam. The images in (a) and (c) show the nanoparticle projections with different shapes and orientations. Therefore, one can use the different shapes and orientations of the nanoparticle projections in Fig. 1b to determine the diffraction spot in the SAED pattern corresponding to each nanoparticle.

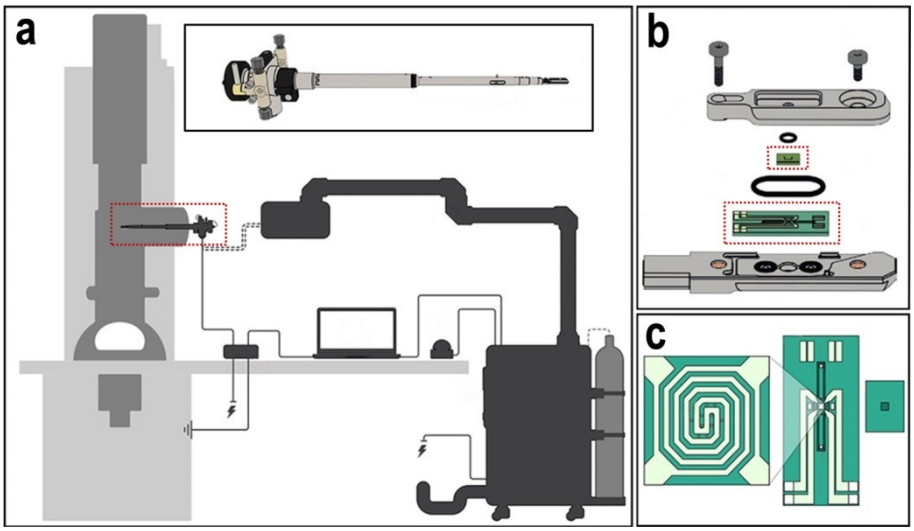

Fig. S2 Schematic diagrams of the *in situ* TEM gas system. (a) Schematic of the TEM, a computer control system, and a gas-supply system; the inset shows an enlarged image of the *in situ* sample holder indicated by the red box in the main panel. (b) Schematic of the sample chamber at the tip of the *in situ* holder. (c) Top-view of the top and the bottom chips, which are indicated by the two red boxes in (b). The enlarged image in (c) is the observation zone when the holder is placed inside the TEM. This system provides an atmospheric-pressure H_2 environment for samples in the observation zone.[21]

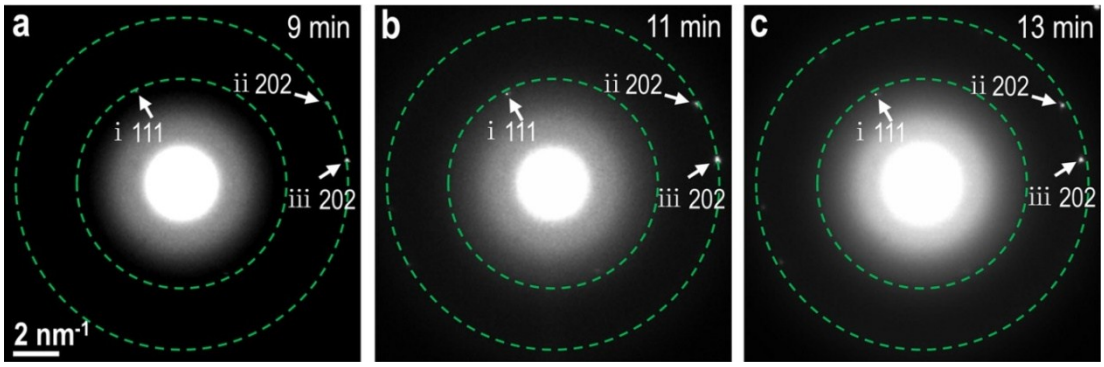

Fig. S3 Evolution of the SAED pattern in Fig. 1b after the corresponding Pd nanoparticles were exposed in the atmospheric-pressure H_2 for 9, 11, and 13 min. The dashed circles in (a-c) are identical, and they are located at the same positions. It can be seen that the positions of the $i_{\{111\}}$, $ii_{\{202\}}$ and $iii_{\{202\}}$ diffraction spots change as the exposure time elapses. By these positions, $d_{\{111\}}$ and $d_{\{220\}}$ were measured to be 0.228 and 0.140 nm at 9 min (a), 0.233 and 0.141 nm at 11 min (b), and 0.233 and 0.144 nm at 13 min (c), respectively.

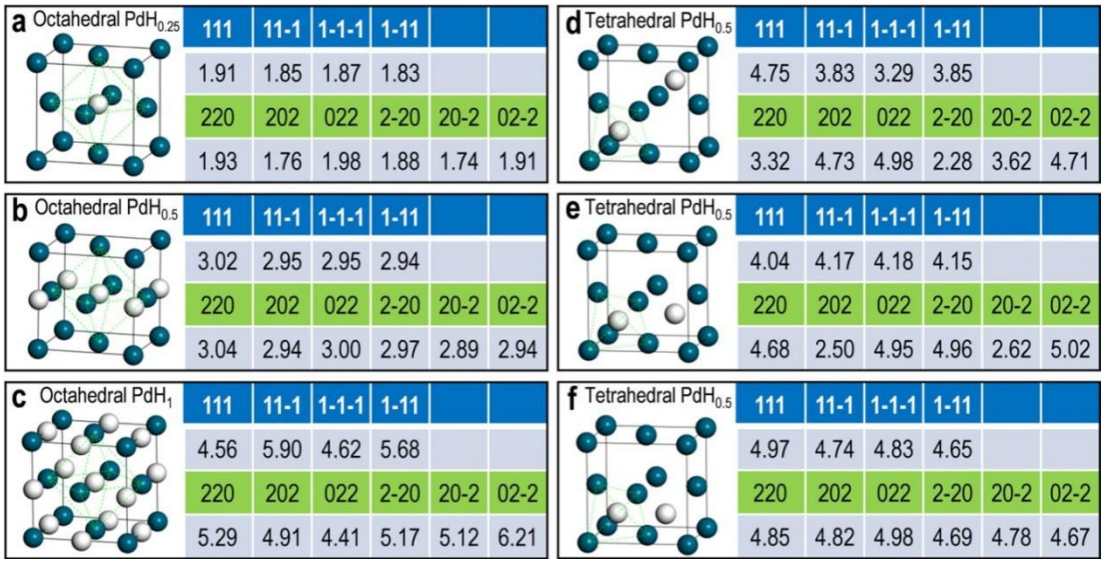

Fig. S4 The models and calculated *d* expansions of PdH_x with H atoms at the OSs or TSs. (a–c) Models of $PdH_{0.25}$, $PdH_{0.5}$, and PdH_1 with H atoms at the OSs and their *d* expansions of {111} and {220}. The values in the grey table cells are the *d* expansions, and their units are all %. (d–f) Three possible models of $PdH_{0.5}$ with H atoms at the TSs and their d expansions of {111} and {220}. The models in (b) and (d–f) are denoted by O, T_1, T_2, and T_3, respectively, in Fig. 2f. It should be noted that upon hydrogen storage, the symmetry of PdH_x becomes lower than that of pure Pd, resulting different expansion values for different {111} planes (such as (111) and (11–1)) or different {220} planes. Therefore, the minimum and maximum values of their d expansion were provided in Fig. 2f.

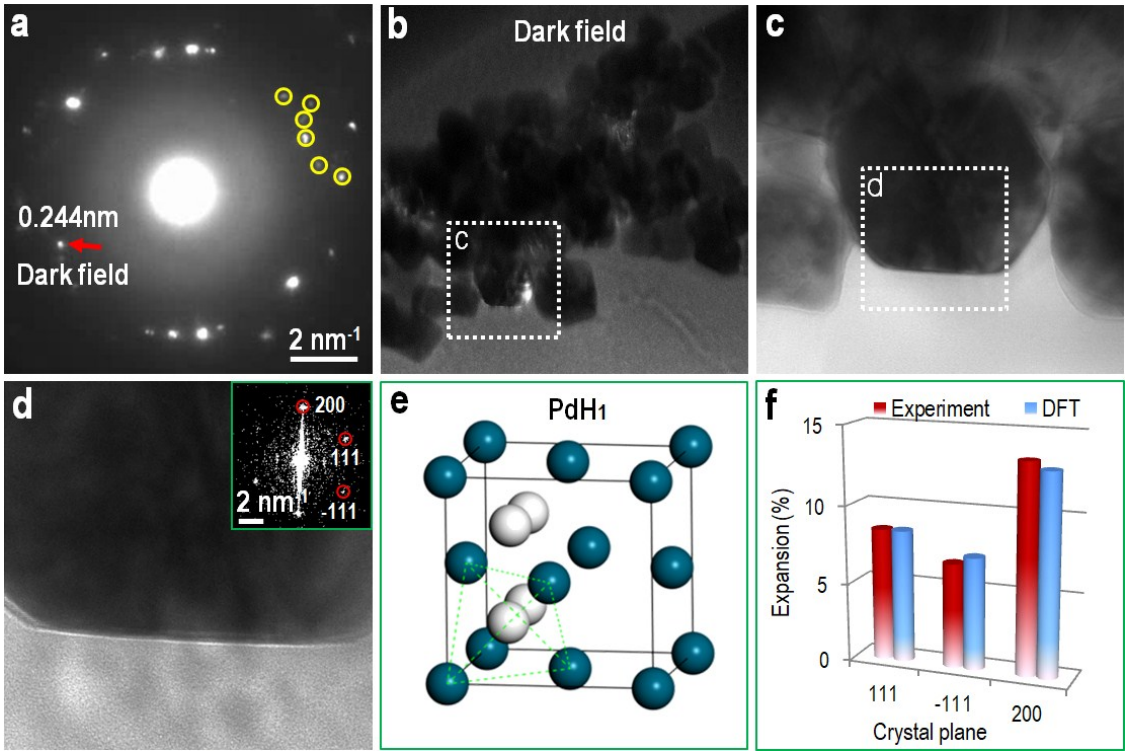

Fig. S5 Different expansion of Pd crystal planes during hydrogen storage. (a) SAED pattern and (b) dark-field image of some Pd nanoparticles. According to SAED pattern, the expansions of {111} are different, as indicated by the yellow circles in (a). There is a diffraction spot for a $d_{\{111\}}$ spacing of 0.244 nm, as indicated by red arrow, meaning the (111) crystal plane expanded by 8.4%. The dark-field image in (b) is obtained from this diffraction spot. This diffraction spot is clearly from the highlighted position, as shown by the box in (b). (c) Bright-field image of the octahedral Pd particle, indicated by the box in (b). (d) HRTEM image and its FFT pattern (inset) of the particle in (c). (e) Model of PdH_1, in which the H atoms occupy tetrahedral positions. (f) Comparison of {111}, {-111}, and {200} expansion according to the FFT pattern in (d) and theoretical model in (e). Significantly, the expansions of {111}, {-111}, and {200} are different even in a single Pd particle when H atoms occupy the tetrahedral positions.

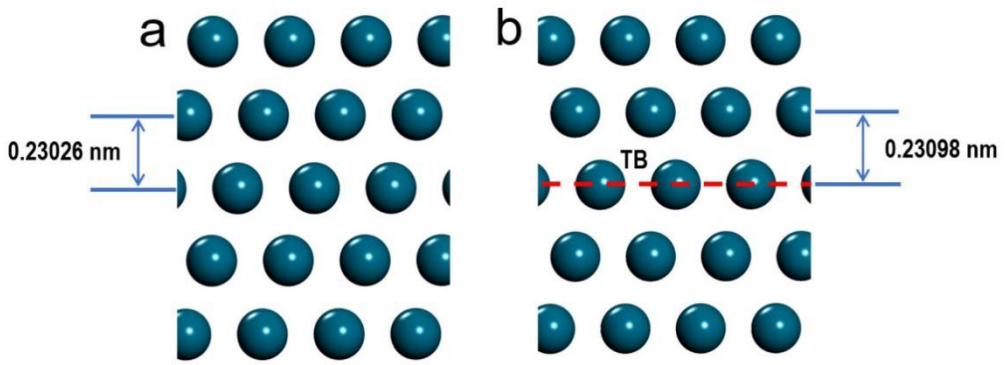

Fig. S6 Interplanar spacing $d_{\{111\}}$ in the Pd matrix, which was the same before and after formation of a stacking fault. TB: twin boundary.

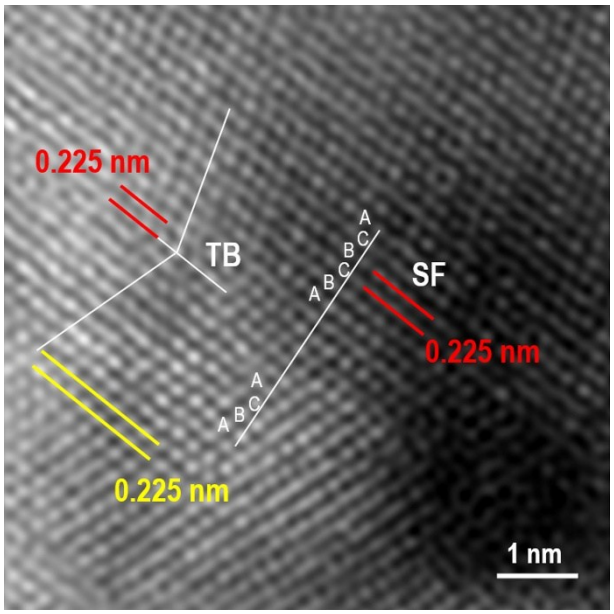

Fig. S7 Twin boundary (TB) and stacking fault (SF) in Pd particles before hydrogen storage. The interplanar spacings of TB and SF were the same as that in the matrix.

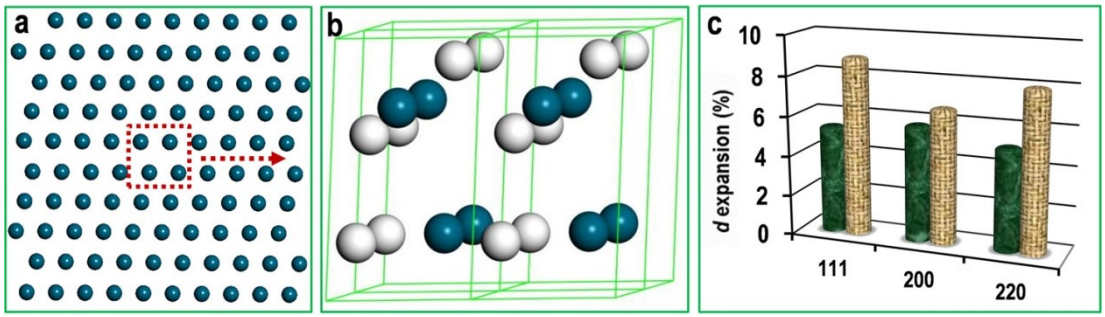

Fig. S8 Model and calculated *d* expansions of $PdH_{1.5}$ of {111} stacking fault. (a) Simulation of {111} stacking fault. (b) Possible model of $PdH_{1.5}$ with H atoms at the {111} stacking fault, which corresponds to the region in the red box in (a). The {111} stacking fault in Pd has a hexagonal closed-packed crystal structure; therefore, these H atoms are stored at similar octahedral and tetrahedral sites. (c) Minimum and maximum values of *d* expansions of {111}, {200}, and {220} according to this model. It should be noted that the range of $d_{\{111\}}$ is 5.4% to 8.9%. For comparison, $d_{\{111\}}$ was found to be 8.2% from the results in Fig. 3, which is in good agreement with the range of *d* shown here.